geosciences

MDPI

Article

Evaluating Sexual Dimorphism in Postcranial Elements of Eurasian Extinct *Stephanorhinus etruscus* (Falconer, 1868) (Mammalia, Rhinocerotidae)

Andrea Faggi and Luca Pandolfi *

Paleo[Fab]Lab, Dipartimento di Scienze della Terra, Università di Firenze, Via G. La Pira 4, 50121 Firenze, Italy; andrea.faggi@unifi.it

* Correspondence: luca.pandolfi@unifi.it

Abstract: Sexual dimorphism has been poorly evaluated or investigated in Pleistocene Eurasian *Stephanorhinus* species, leaving a gap in our knowledge about their morphometric variability. Among the representatives of this genus, *S. etruscus* is the most abundant species, with several remains collected from Western European localities, allowing us to investigate the presence of sexual dimorphism in the limb bones of this taxon. We considered measurements taken on 45 postcranial variables and three different statistical metrics to identify patterns of bimodality in the dataset. This work represents the first application of sex-combined statistical analysis to a dataset composed of individuals from various European localities. The morphometrical analyses revealed that a relatively weak sexual dimorphism is present in all the considered bones. Larger forelimbs and hindlimbs are interpreted as belonging to adult males of *S. etruscus*, similarly to what was observed in the modern Sumatran rhino, where males are a little bit larger than females. The recognition of a weak sexual dimorphism in the postcranial bones of *S. etruscus* increases our understanding of the paleoecology of this extinct taxon. However, only a better study of the morphological and morphometrical variability of the crania of fossil rhinoceroses could deeply contribute to the investigation of the social habits and behavior of these taxa.

Keywords: sexual dimorphism; analytic tools; rhinoceroses; Eurasia; Quaternary

Citation: Faggi, A.; Pandolfi, L. Evaluating Sexual Dimorphism in Postcranial Elements of Eurasian Extinct *Stephanorhinus etruscus* (Falconer, 1868) (Mammalia, Rhinocerotidae). *Geosciences* **2022**, *12*, 164. https://doi.org/10.3390/geosciences12040164

Academic Editors: Angelos G. Maravelis and Jesus Martinez-Frias

Received: 26 February 2022
Accepted: 4 April 2022
Published: 7 April 2022

1. Introduction

Sexual dimorphism represents a common feature of many mammals, and it affects the body size and morphometry of several species [1–4]. The family Rhinocerotidae displays a certain degree of sexual dimorphism in extant and fossil species. Among the extant rhinoceroses, Groves [5] detected dimorphic characters in the width of the nasal bones, the height of the occiput, and the width of the mastoids on the crania of the Indian rhinoceros (*Rhinoceros unicornis*). Guérin [6] and Groves [5] documented a larger size of female individuals in respect to males in *Rhinoceros sondaicus*. The scant available samples analysed by the above-mentioned authors suggested that males and females of *R. sondaicus* display a large overlap in nasal width, but with males having a well-developed horn [5,7]. According to Pocock [7] and Groves [5], nasal width differs in males and females of *Dicerorhinus sumatrensis*, at least in the mainland and Sumatran forms but not in the Bornean subspecies (cf. [5]). Furthermore, wild Sumatran rhinoceros males are proportionally larger than females [5]. Owen-Smith [8] pointed out that *Ceratotherium simum* (the white rhino) is sexually dimorphic in body size and horn size whereas *Diceros bicornis* (the black rhino) is monomorphic. According to Rachlow and Berger [9], adult male white rhinos have larger horn bases than adult females.

Sexual dimorphism has been documented in cranial remains of some Neogene Rhinocerotidae lineages [10–20]. The early Miocene *Menoceras arikarense* shows horn bosses with a degree of dimorphism comparable to modern ruminants [17,19]. Individuals of the

North American genera *Teleoceras* and *Aphelops* can be easily distinguished in male and female groups based on tusk size [12,14–16,18]. In Eurasia, Cerdeño and Sánchez [20] detected sexual dimorphism in the development of i2, as tusks, in *Alicornops simorrensis* and *Aceratherium incisivum*. Deng [10] and Chen et al. [21] observed that male individuals of *Chiloterium wimani* had bigger tusks, more robust mandibles, and wider skulls than females. In the elasmotherine *Iranotherium morgani*, Deng [11] discovered one qualitatively dimorphic character (males have a hemispherical hypertrophy on zygomatic arches while female individuals have no such structure) and several quantitative sexually dimorphic characters in the development of the nasal horn boss, in the width of the zygomatic arches, and in the width of the anterior part of the nasals. Lu et al. [13] noted that in *Plesiaceratherium gracile* both lower tusks and upper incisors are sexually dimorphic. Lastly, Borsuk-Bialynicka [22] discovered that several cranial dimensions of *Coelodonta antiquitatis* were bimodal (such as the width of occiput, the maximum length, the orbit–nuchal crest, the orbit–nares lengths, and the width of the zygomatic arches). Studies on dimorphic characters in postcranial remains, which are often the most abundant element in the Rhinocerotidae fossil record, are currently limited to a few North American taxa [15–17,23], and no studies have been previously conducted on this topic within Quaternary species.

Although some research on cranial material has been carried out [24–26], sexual dimorphism has been poorly evaluated or investigated in Pleistocene Eurasian *Stephanorhinus* species, leaving a gap in our knowledge about their morphometric variability. Among the representatives of this genus, *S. etruscus* represents the most abundant species, with numerous remains collected from Western European localities. The aim of this contribution is therefore to detect possible sexual dimorphic characters in the measurements of postcranial material referred to the extinct *S. etruscus*.

2. Materials and Methods

We considered measurements taken on 45 postcranial variables of main weightbearing limb elements including radius, third metacarpal (MCIII), tibia, astragalus, calcaneum, and third metatarsal (MTIII). The humerus and femur of *S. etruscus* were not included in this study; despite being good indicators of dimorphism, these two bones are often damaged and/or deformed. Linear measurements and bone circumferences were collected by direct study of material housed in various European institutions and from published material (Supplementary Materials S1 and S2). All the considered limb bones belong to adult individuals with completely fused epiphyses. Because of the disarticulated nature of *S. etruscus* remains, it was impossible to determine the sex of the material a priori in any postcranial element. Therefore, it was necessary to apply different methods. Mihlbachler [16,17] found that sex-combined summary statistics were capable of pinpointing strong sexual dimorphism, identifying patterns of bimodality in the sex-combined assemblage of bones against the null expectation of a unimodal normal distribution. Three different statistical metrics were used to identify patterns of bimodality in the data: (1) in mammals, sexually dimorphic variables, such as tusks in *Teleoceras* [15,17], tend to yield coefficients of variation that exceed a value of 10 [27]; (2) a Shapiro–Wilk test of normality (W) was used to test for deviation from a unimodal normal distribution. Significant results indicate deviation from normality. Sall & Lehman [28] recommended an alpha level (p) for this test < 0.1; (3) an additional mean to verify the presence of dimorphism is the coefficient of bimodality (b). A value of b greater than 0.55 usually indicates a bimodal or polymodal distribution [29,30]. The Shapiro–Wilk test of normality was developed in R Environment version 3.6.1 [30] with the package *stats*(), version 3.6.1. The bimodality coefficient b was developed in R Environment version 3.6.1 [31] with the package *mouse trap*() version 3.1.5 [32]. All graphs were obtained in R Environment version 3.6.1 (2019) [31] with the package *ggplot2*() version 3.3.3 [33]. Mathematical equations used to calculate statistical metrics can be found in Supplementary Materials S3.

Measurement abbreviations: APDb, calcaneum anterior–posterior diameter of the beak; APDm, astragalus anterior–posterior diameter of the medial face; APDS, anterior-

posterior diameter of the shaft; APDs, calcaneum anterior–posterior diameter of the tuber calcanei; DAPD, anterior–posterior diameter of the distal epiphysis; DAPDa, anterior–posterior diameter of the distal articular surface; DTD, transverse diameter of the distal epiphysis; DTDa, transverse diameter of the distal articular surface; Hm, height of the medial face of astragalus; Hmax, maximum height; Hl, height of the lateral face of astragalus; Htm, height of the medial lip of the trochlea; Htl, height of the lateral lip of the trochlea; Lmax, maximal length; PAPD, anterior–posterior diameter of the proximal epiphysis; PTD, transverse diameter of the proximal epiphysis; TDl, transverse diameter between the lips of the trochlea; TDmax, astragalus maximum transverse diameter; TDmp, calcaneum minimum posterior transverse diameter; TDS, transverse diameter of the shaft; TDs, calcaneum transverse diameter of the tuber calcanei; TDst, transverse diameter of the sustentaculum talii.

Other abbreviations: CV, coefficient of variation; max, maximum; min, minimum; N, number of observations; Pr. < W, p value for Shapiro–Wilk test of normality; SD, standard deviation.

3. Results

Specimens from Upper Valdarno are well-represented within the considered dataset; accordingly, a statistical analysis and a graphical representation of this sample have been attempted (Supplementary Materials S2). Bivariate plots of selected measurements, such as the Lmax, DTD and DTP, show the presence of two possible clusters in the radius, tibia, MCIII, and MTIII (Supplementary Material S3: Figures S1–S6). However, statistical metrics were not able to identify a clear bimodal distribution due to the low number of values (Supplementary Materials S3: Tables S1–S6).

Considering the dataset as a whole, four measurements on 45 (9%) show a bimodality coefficient (b) greater than or equal to 0.55, and six others are very close to this value. Eight measurements (18%) have a high coefficient of variation (CV > 10) and 16 (35%) deviate from the normal trend of the distribution curve (p-value < 0.1), suggesting that some postcranial characters of *S. etruscus* are bimodal.

A closer look at the postcranial data reveals which postcranial variables have a higher probability to be sexually dimorphic. Only the APDS of the radius (Table 1) yields a coefficient of bimodality higher than 0.55. The same variable shows a relatively high coefficient of variation.

Table 1. Sex-combined statistics for radius variables.

Variable	Mean	SD	Min.	Max.	N	CV	b	Pr < W
Lmax	374.168	29.23737	328.52	384.9	9	7.813951	0.279	0.4068
PTD	86.6676	3.845524	74	92	21	4.437094	0.442	**0.00654**
PAPD	59.0118	4.404664	46.5	66.8	22	7.464038	0.263	0.2037
TDS	46.1010	3.156613	39.5	54	19	6.847161	0.394	0.2897
APDS	36.955	3.871884	28.68	41.46	14	**10.47729**	**0.55**	0.124
DTD	85.4025	3.802879	77.9	94	12	4.452890	0.313	0.6228
DAPD	56.2488	5.654382	50.7	69	9	**10.05243**	0.417	**0.0445**

Abbreviations: SD, standard deviation; min., minimum; max. maximum; N, number of observations; CV, coefficient of variation; b, coefficient of bimodality; Pr < W, probability value of Shapiro–Wilk test of univariate normality. Variables that exceed the threshold are in bold.

The DAPD has a relatively high coefficient of variation and deviates significantly from normality, similarly to PTD. Concerning the results obtained for the tibia (Table 2), it is possible to observe that only the PTD passes all three tests and shows a low p-value for the Shapiro–Wilk test of normality, indicating a strong deviation from normality.

Table 2. Sex-combined statistics for tibia variables.

Variable	Mean	SD	Min.	Max.	N	CV	b	Pr < W
Lmax	357.665	19.42609	327	384	16	5.343678	0.487	**0.091**
PTD	104.135	11.87361	78	117	19	**11.40213**	**0.552**	**0.009**
PAPD	112.6207	5.522146	103.2	115.2	15	4.903315	0.319	0.289
TDS	52.435	2.689569	46	56	28	5.129339	0.478	**0.044**
APDS	49.38647	5.612956	41	62	18	**11.36537**	0.359	0.562
DTD	87.52621	7.477514	73.3	108	29	8.543172	0.328	0.278
DAPD	62.3169	4.156129	55	70.4	30	6.669345	0.383	0.757

Abbreviations as in Table 1. Variables that exceed the threshold are in bold.

Moreover, the APDS also yields a high coefficient of variance, while the Lmax and TDS deviate significantly from normality and have relatively high (≈0.5) coefficients of bimodality. For the astragalus (Table 3) and calcaneum (Table 4), despite the high number of measurements, coefficients of variation are rather low and only one measurement, Hmax, yields a high coefficient of bimodality.

Table 3. Sex-combined statistics for astragalus variables.

Variable	Mean	SD	Min.	Max.	N	CV	b	Pr < W
TDmax	81.0555	4.233048	73	88	40	5.222407	0.34	**0.07**
Hm	68.88423	3.186718	62.23	75	26	4.626193	0.377	0.93
DAPDa	42.83813	2.78072	35.84	46.36	16	6.491227	0.24	0.12
DTDa	66.30423	4.285001	58	72	26	6.462636	0.502	**0.046**
TDl	54.39519	4.408431	48	61.5	27	8.104451	0.502	**0.063**
DTD	68.52541	4.731199	58	78	37	6.904299	0.4	0.44
Hl	71.20308	2.557828	65.78	76.7	26	3.5923	0.32	0.84
DAPD	41.22036	2.946914	36	47	29	7.149171	0.316	0.64
Htm	54.10913	6.851269	41.2	63	24	**12.66195**	0.52	**0.031**
APDm	50.14744	4.640133	37.5	56.97	39	9.252981	0.47	**0.033**
Htl	58.41789	3.375294	53.22	64.2	19	5.777842	0.43	0.39
Hmax	74.01879	5.928035	58	84	33	8.008825	0.41	0.34

Abbreviations as in Table 1. Variables that exceed the threshold are in bold.

Table 4. Sex-combined statistics for calcaneum variables.

Misura	Media	SD	Min.	Max.	N	CV	b	Pr < W
Hmax	117.4142	5.18844	105	123	26	4.41892	**0.61**	**0.003**
APDs	63.61185	4.50524	52.5	71	27	7.08239	0.37	0.14
TDs	43.68462	2.565859	39.2	48	26	5.873599	0.42	**0.088**
APDb	60.04321	5.032526	50	68.4	28	8.381507	0.29	0.6
TDst	70.68565	4.560885	60	76.19	23	6.452349	0.52	**0.042**
TDmp	34.05148	3.279682	25.4	39.16	27	9.631539	0.4	0.32

Abbreviations as in Table 1. Variables that exceed the threshold are in bold.

However, eight measurements in the astragalus and calcaneum deviate considerably from a normal distribution. This could be due to the presence of a weak signal of dimorphism, supported also by a relatively high (≈0.5) coefficient of bimodality, or to the presence of some outliers in the dataset. In the third metatarsals (Table 5) the DTD passes all three tests, while the APDs of proximal and distal epiphyses have a high coefficient of variation; other measurements such as APDS and Lmax have a coefficient of variation close to 10 and, just for Lmax, a relatively high coefficient of bimodality, possibly indicating a faint signal of bimodality. In the third metacarpal (Table 6), only the Lmax and the PTD deviate significantly from the normal distribution, with Lmax having a relatively high coefficient of bimodality.

Table 5. Sex-combined statistics for third metatarsal variables.

Variable	Mean	SD	Min.	Max.	N	CV	b	Pr < W
Lmax	171.7639	10.69157	152.18	186	18	9.677419	0.533	0.2184
DTD	49.6685	5.123739	38	55	20	**10.31587**	**0.633**	**0.0034**
TDS	40.72708	3.234339	33	48.94	24	7.941496	0.222	0.2821
PTD	47.66179	3.157637	40.36	52.35	28	6.625093	0.387	0.4216
PAPD	40.228	4.644855	29	48.83	20	**11.54632**	0.24	0.5871
DAPD	35.96105	3.585777	27.71	44	19	**10.0000**	0.226	0.3462
APDS	21.62391	2.040418	16.68	25	23	9.435934	0.323	0.5977

Abbreviations as in Table 1. Variables that exceed the threshold are in bold.

Table 6. Sex-combined statistics for third metacarpal variables.

Variable	Mean	SD	Min.	Max.	N	CV	b	Pr < W
Lmax	192.3784	8.544863	179.12	203.97	18	4.438646	0.541	**0.02388**
DTD	56.1685	2.584509	51.66	60	20	4.601349	0.419	0.2127
TDS	46.9508	2.280907	43.4	51.32	25	4.858081	0.379	0.3772
PTD	50.9152	3.298375	42	57.09	24	6.625092	0.414	**0.007299**
PAPD	44.2988	1.967814	40.07	49	18	4.442129	0.210	0.7993
DAPD	39.83230	1.552251	37.2	42	13	3.896969	0.359	0.7297
APDS	19.2525	1.551084	16.4	21.89	19	8.056533	0.410	0.4253

Abbreviations as in Table 1. Variables that exceed the threshold are in bold.

Frequency histograms and bivariate plots of postcranial dimensions are shown in Figures 1–12. Using these two types of visual representation, it is easier to observe the bimodal distribution in the dataset. Due to the small number of complete specimens, the values collected from the radius are too scattered to be grouped in two clusters (Figure 7). Histograms of tibia's Lmax, calcaneum's Hmax and metapodials' Lmax (Figures 2 and 4–6) show that there are two different values around which the measurements are distributed, while the histogram on astragalus (Figure 3) shows a less evident bimodal distribution. Bivariate plots (Figures 7–12) allow better underlining of the presence of two clusters, in particular for the astragalus, calcaneum, and MTIII (Figures 9, 10 and 12). The tibia and MCIII bivariate plots (Figures 8 and 11) suggest the presence of two different clusters, but in both cases the cluster made up of the smallest individuals contains only a few specimens.

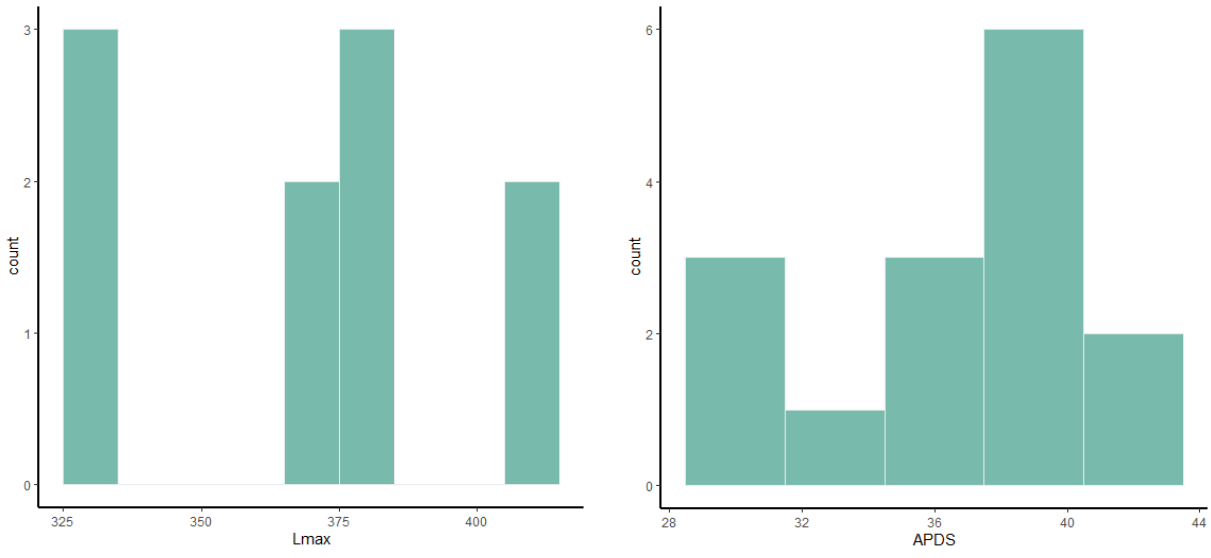

(**a**) (**b**)

Figure 1. (**a**) Frequency distribution of the maximum length (Lmax) and (**b**) the anterior–posterior diameter of the shaft in the radius of *S. etruscus*.

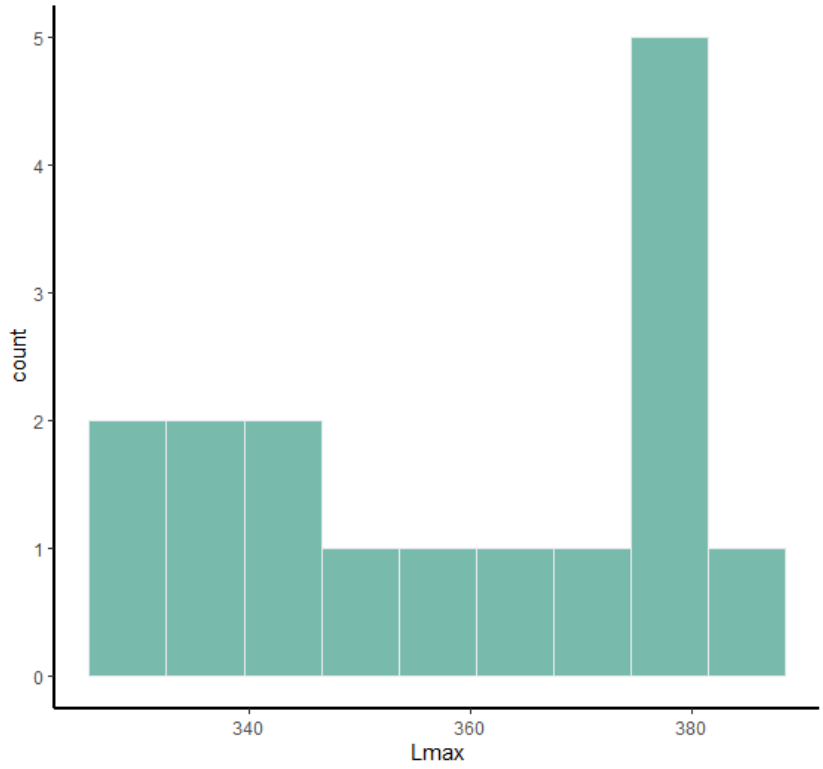

Figure 2. Frequency distribution of the maximum length (Lmax) in the tibia of *S. etruscus*.

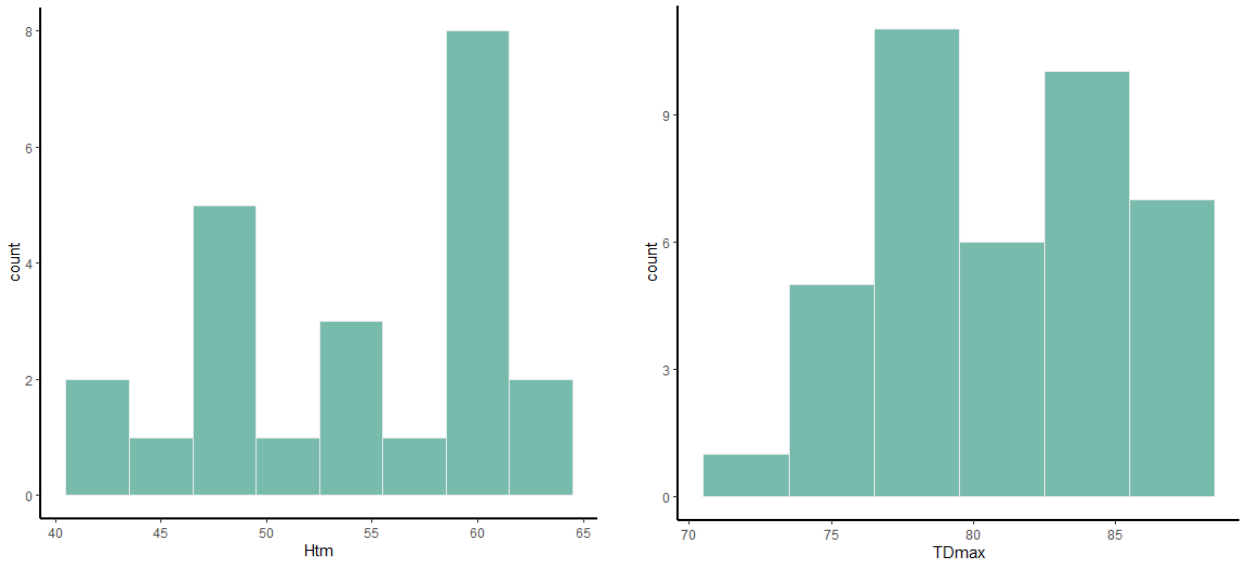

(**a**) (**b**)

Figure 3. (**a**) Frequency distribution of the height of the trochlea's medial lip (HTm) and (**b**) the maximum transverse diameter in the astragalus of *S. etruscus*.

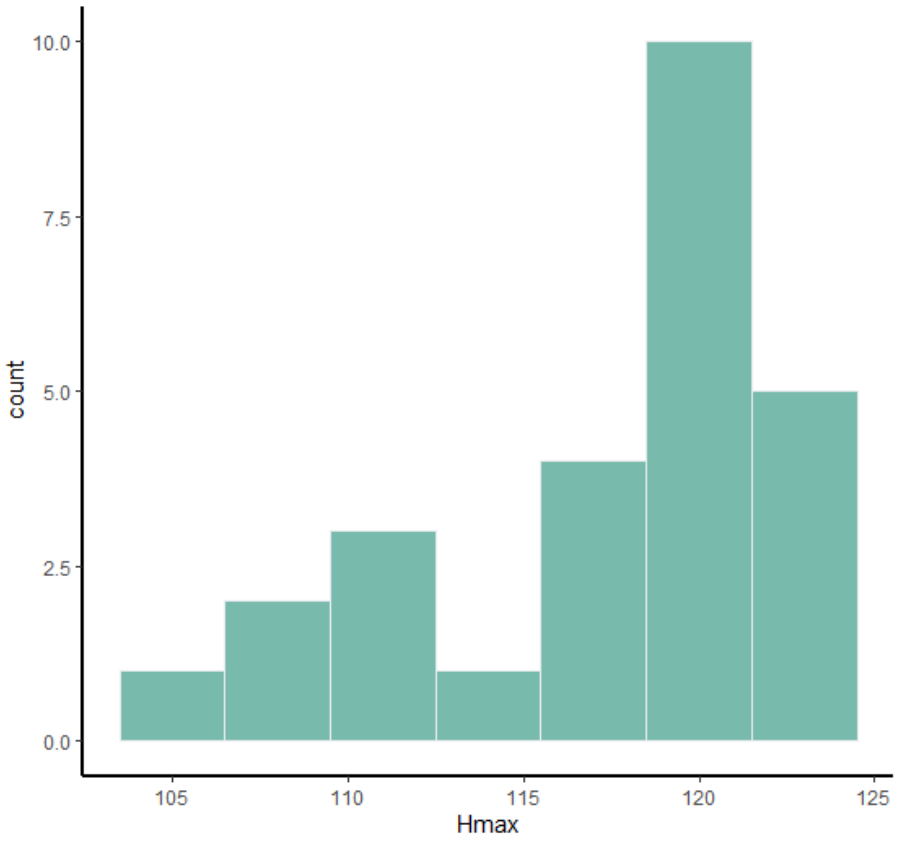

Figure 4. Frequency distribution of the maximum height (Hmax) in the calcaneum of *S. etruscus*.

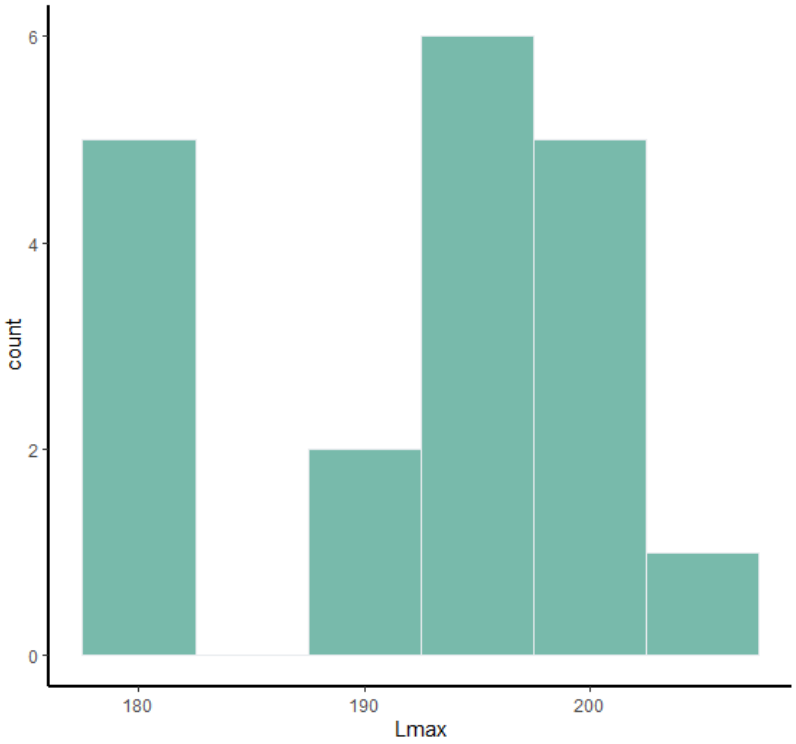

Figure 5. Frequency distribution of the maximum length (Lmax) in the MCIII of *S. etruscus*.

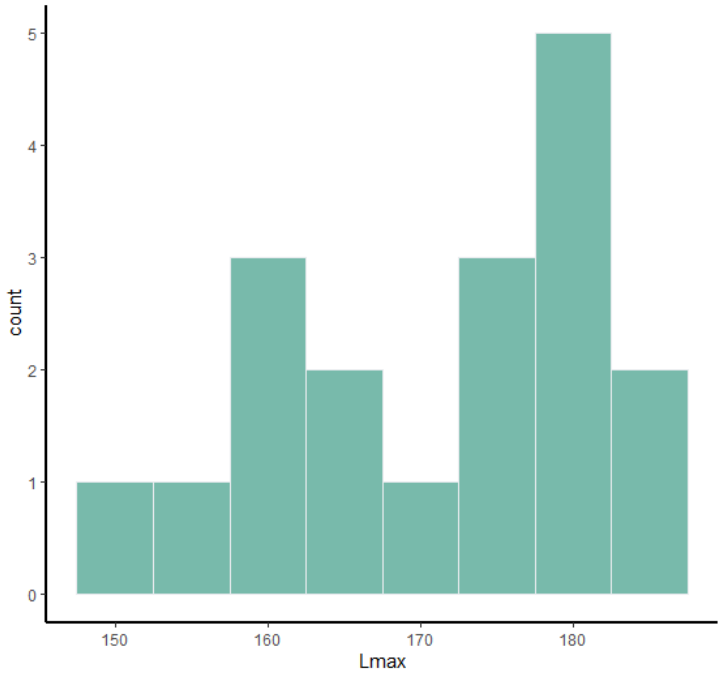

Figure 6. Frequency distribution of the maximum length (Lmax) in the MTIII of *S. etruscus*.

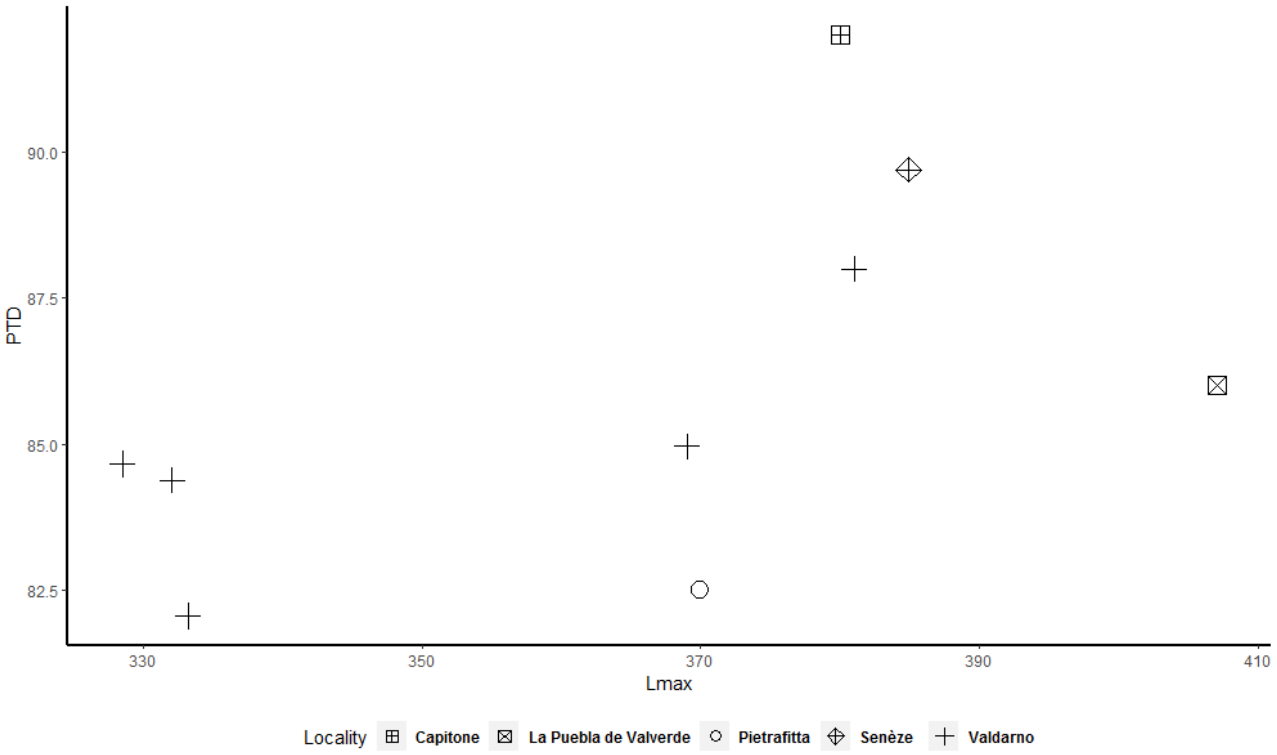

Figure 7. Scatterplot between the maximum length (Lmax) and the proximal transverse diameter (PTD) of the radius.

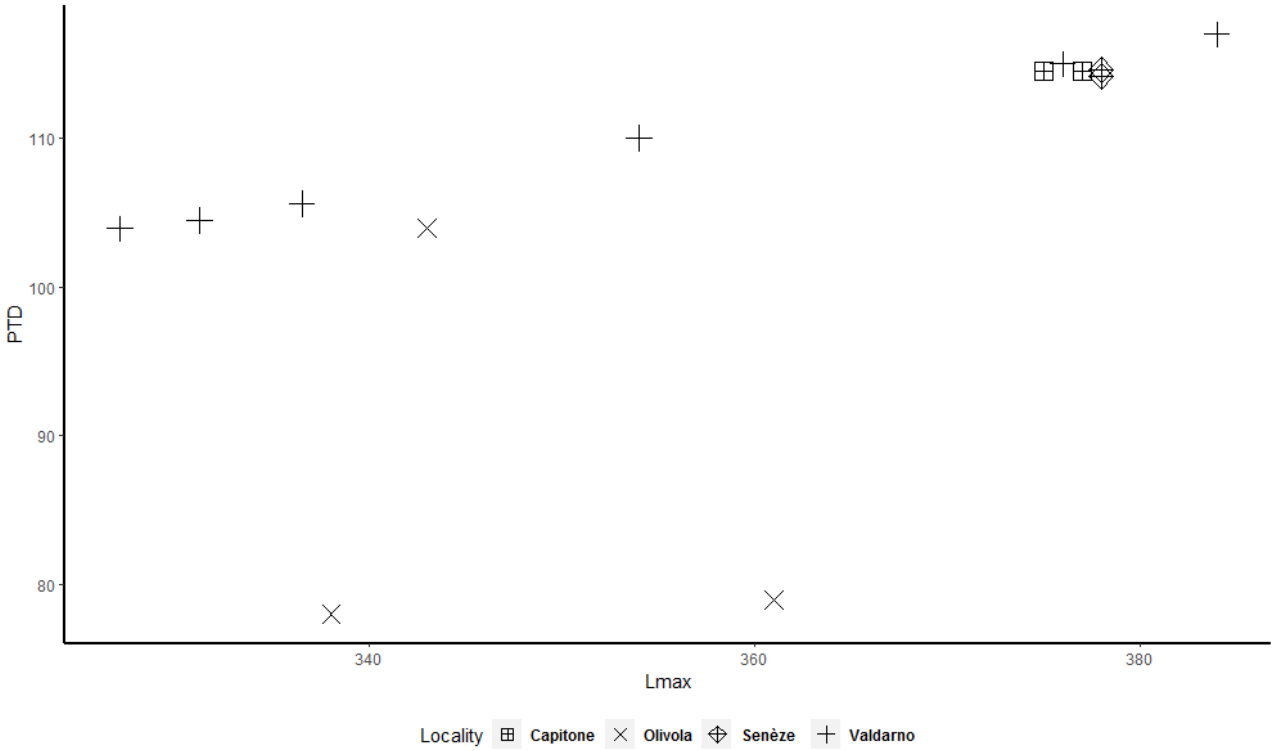

Figure 8. Scatterplot between the maximum length (Lmax) and the proximal transverse diameter (PTD) of the tibia.

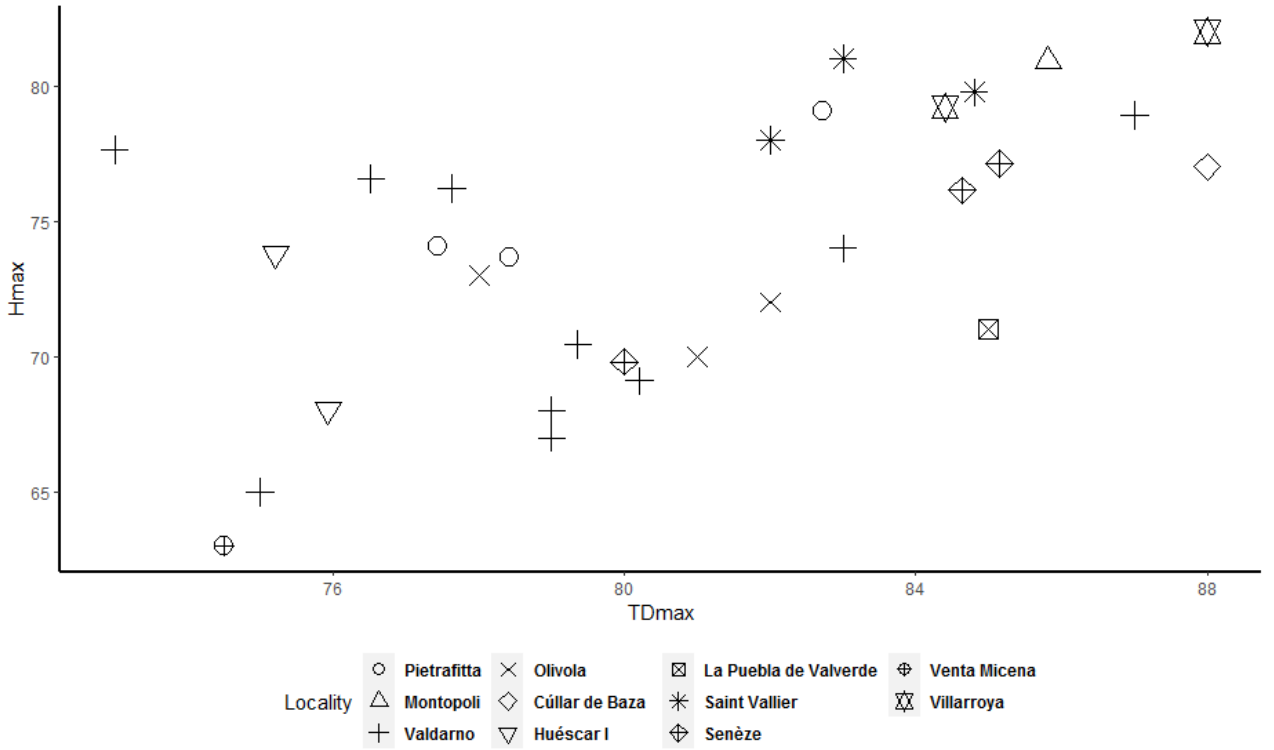

Figure 9. Scatterplot between the maximum transverse diameter (Tdmax) and the maximum height (Hmax) of astragalus.

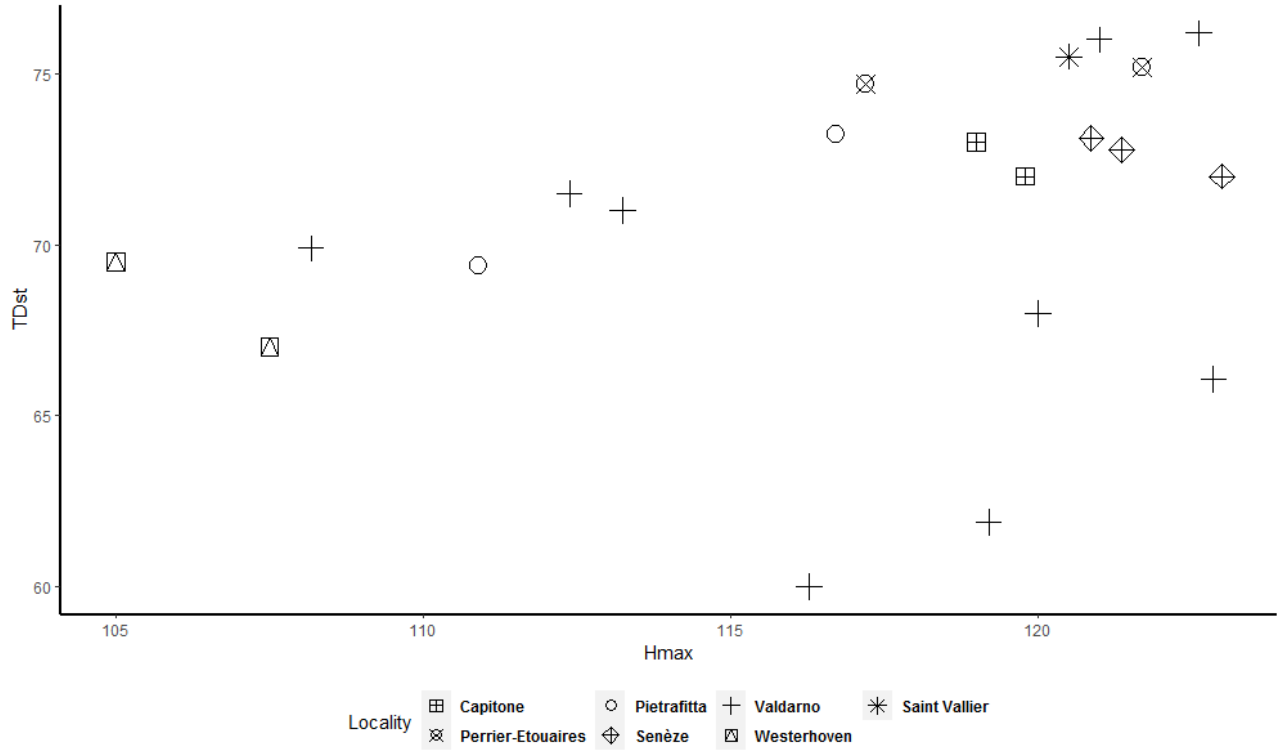

Figure 10. Scatterplot between the maximum height (Hmax) and the transverse diameter of the sustentaculum talii (TDst) of the calcaneum.

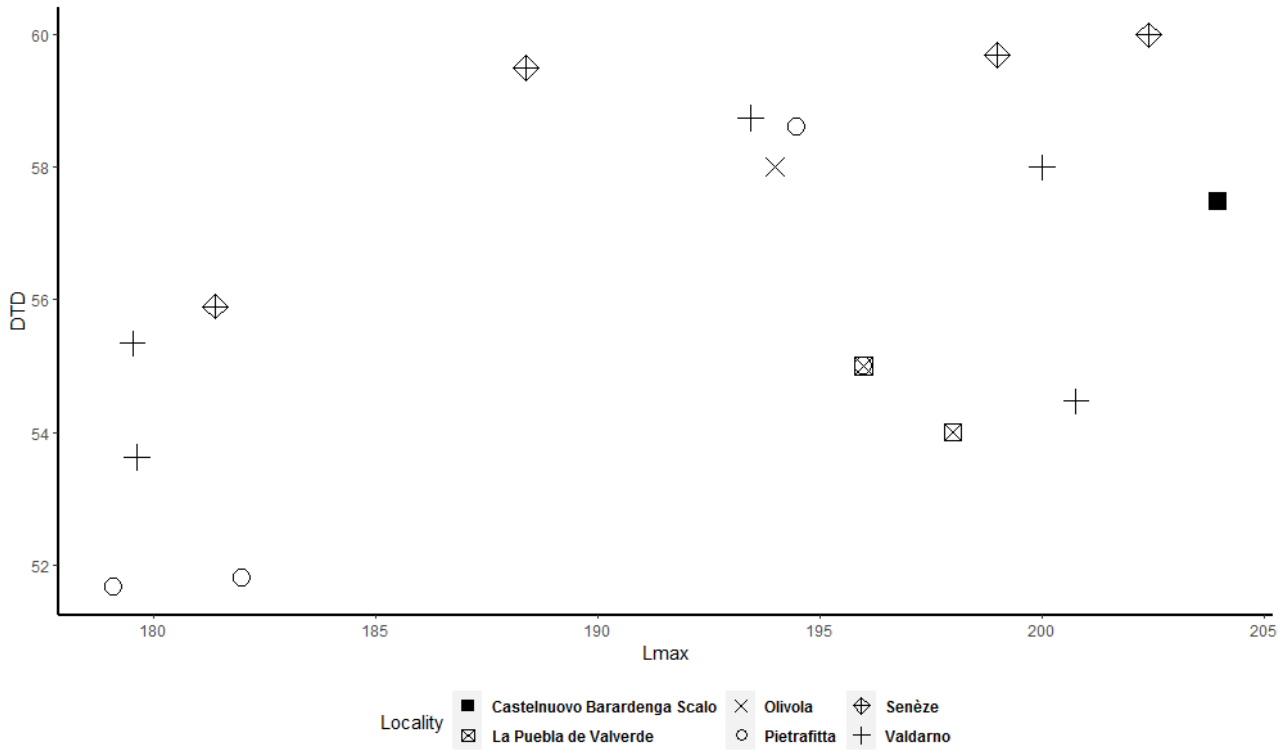

Figure 11. Scatterplot between the maximum length (Lmax) and the distal transverse diameter (DTD) of the MCIII.

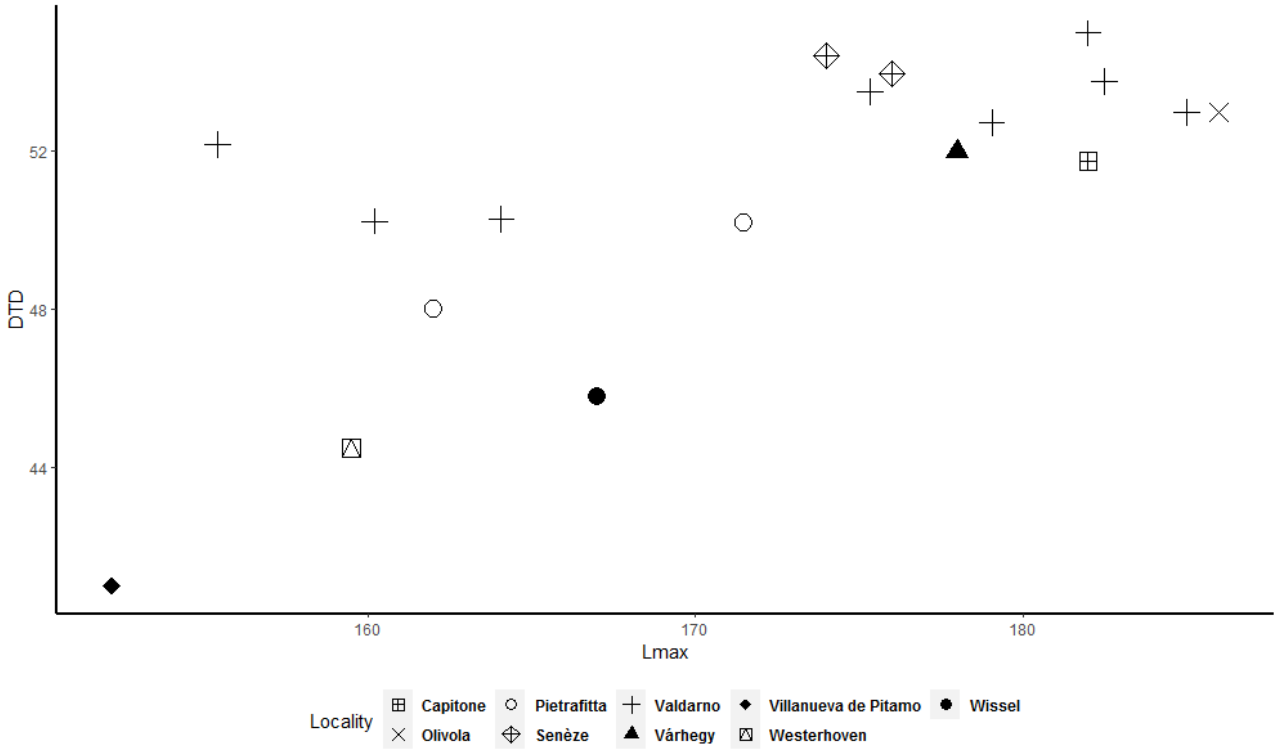

Figure 12. Scatterplot between the maximum length (Lmax) and the distal transverse diameter (DTD) of the MTIII.

4. Discussion

Three sex-combined statistical methods allowed us to detect a weak signal of sexual dimorphism for each considered postcranial element of *S. etruscus*. The results that indicate a possible bivariate distribution for each statistical analysis and for each postcranial element are summarized in Table 7.

Table 7. Summary table of the number of variables that exceed the limit value for each statistical analysis.

Bone	CV	b	Pr < W
Radius	2(1)	1	2(1)
Tibia	2	1	3
Astragalus	1(1)	0(3)	5(1)
Calcaneum	0(1)	1(1)	3(1)
MCIII	0	0(1)	2
MTIII	3(2)	1(1)	1

Abbreviations: CV, coefficient of variation; b, coefficient of bimodality; Pr < W, probability value of Shapiro–Wilk test of univariate normality. Variables that are very close to the limit value are shown in brackets (9 < CV < 10; 0.5 < b < 0.55; 0.1 < PrW < 0.2).

The presence of sexual dimorphism in fossil Rhinocerotidae has been investigated primarily on cranial remains [10–18,22], but little has been done on the variability of the postcranial elements [13,15–17]. This is mainly related to the frequently disarticulated nature of the remains and the need of a large dataset for comparison. Mead [15] observed that the Miocene rhinoceros *Teleoceras major* from the Ashfall beds shows a high degree of dimorphism in both the anterior and posterior limbs. Mihlbachler [16], using sex-combined summary statistics, confirmed the presence of sexual dimorphism in the postcranial elements of *Teleoceras major* and observed it for the first time in *Teleoceras proterum* and *Aphelops malacorhinus*. Mihlbachler [17] investigated the presence of sexual dimorphism in the limbs of *M. arikarense* but did not find any clear evidence of sex variance. Lastly, Lu et al. [13]

suggested that female individuals of *P. gracile* were longer and taller while male individuals were generally smaller but more robust.

Pleistocene *Stephanorhinus* species have been the subject of numerous morphological and morphometric studies in Europe, but only a few of them discussed the presence of sexually dimorphic characters, in particular on cranial remains. Thenius [34] suggested that there are a few adult specimens of the Etruscan rhinoceros in which the nasal septum is not ossified, probably representing females. A distinction between males and females in *Stephanorhinus* was then suggested on the basis of the nasal width [35]. To the contrary, Loose [24] reported that the variability of nasal horns is so large that it is impossible to correlate its development with the sex of the animal. No inquiry was made into postcranial remains [22].

Due to its abundance and geographic distribution [36], *S. etruscus* is the Quaternary Eurasian *Stephanorhinus* that is best suited to be tested for sexual dimorphism.

Here, using sex-combined summary statistics, we detected the presence of a bimodality distribution for some measurements in all of the considered bones (Tables 1–6). The total length of the bones and the diameters of the epiphyses are the measurements that are more often bimodal or at least weakly bimodal. The astragalus (Table 3) and calcaneum (Table 4) are weakly bimodal in some characters such as Tdmax, DTDa, TDl, Htm, and APDm for the astragalus and Hmax, TDs, and TDst for the calcaneum. Even though it was impossible to determine the sex of the studied material a priori, the use of frequency histograms (Figures 1–6) and, above all, bivariate plots (Figures 7–12) shows that two clusters exist among the considered specimens. Bivariate plots can represent the bimodality signal obtained through the use of sex-combined summary statistics, highlighting that some adult individuals were taller and more robust than others.

More importantly, we observed that some adult specimens collected from the same locality, and therefore geographically and temporally close to each other, are plotted in two different clusters and are, in many cases, widely separated (Figures 7–12). As a result, individuals from Valdarno (the most frequently represented locality in the dataset and the type area of the species), Pietrafitta, Olivola, and Senèze suggest that morphometrical variation attributable to sexual dimorphism is not overshadowed by the variability related to the geographical and temporal distribution of the species. However, the analysis of the Valdarno sample only (Supplementary Materials S2) did not strongly support the bimodality patterns observed through bivariate plots (Tables S1–S6) due to the too small number of observations. Only a few measurements (e.g., DTD of MTIII) are indeed statistically significant.

Accordingly, we can assume that *S. etruscus* shows a relatively weak degree of sexual dimorphism in the limbs' dimensions. In extant Indian, Sumatran, African [8,9,37–39], and fossil [15,16,18] Rhinocerotidae, males are larger than females; thus it is possible to hypothesize that in *S. etruscus* males were also slightly larger than females.

5. Conclusions

The abundance of *S. etruscus* in the fossil record allows us to investigate the presence of sexual dimorphism in the limb bones of this taxon. Moreover, the present work represents the first application of sex-combined statistical analysis to a dataset composed of individuals from various European localities. The morphometrical analyses revealed that quantifiable relatively weak sexual dimorphism is present in all the considered bones (Tables 1–6). Adult *S. etruscus* males probably exhibited slightly larger forelimbs and hindlimbs than females; *S. etruscus*, similarly to African rhinos, had extremely reduced or absent incisors [36], and it is therefore logical to assume that males confronted each other using their horns.

However, the results obtained for the Valdarno dataset demonstrated the limits of the applied statistical methods.

The recognition of a relatively weak sexual dimorphism in the postcranial bones of *S. etruscus* furthers our understanding of the paleoecology of this extinct taxon. However, only a better study of the morphological and morphometrical variability of the cranium

of this fossil rhinoceros could deeply contribute to the investigation of the sociability and behavior of the species.

Supplementary Materials: The following supporting information can be downloaded at: https://www.mdpi.com/article/10.3390/geosciences12040164/s1, Supplementary Material S1. Supplementary Material S2, Analysis on Upper Valdarno specimens. Supplementary Material S3, Statistical methods applied on the considered sample. References [25,40–46] are cited in the Supplementary Materials.

Author Contributions: Conceptualization, L.P. and A.F.; methodology, L.P. and A.F.; software, A.F.; validation, L.P. and A.F.; formal analysis, A.F.; investigation, L.P.; resources, L.P. and A.F.; data curation, L.P. and A.F.; writing—original draft preparation, L.P. and A.F.; writing—review and editing, L.P.; visualization, L.P. and A.F.; supervision, L.P.; project administration, L.P.; funding acquisition, L.P. All authors have read and agreed to the published version of the manuscript.

Funding: L.P. thanks the European Commission's Research Infrastructure Action, EU-SYNTHESYS project AT-TAF-2550, DE-TAF-3049, GB-TAF-2825, HU-TAF-3593, HU-TAF-5477, ES-TAF-2997; part of this research received support from the SYNTHESYS Project, http://www.synthesys.info/ (2013–2016, accessed on 15 February 2022) which is financed by European Community Research Infrastructure Action under the FP7 "Capacities" Program. This paper has been developed within the research project "Ecomorphology of fossil and extant Hippopotamids and Rhinocerotids" granted to L.P. by the University of Florence ("Progetto Giovani Ricercatori Protagonisti" initiative).

Institutional Review Board Statement: Not applicable.

Informed Consent Statement: Not applicable.

Data Availability Statement: Not applicable.

Acknowledgments: We thank all the curators of the involved and cited Museum and Institutions. In addition, we thank the Editorial Office of the Journal as well as three Reviewers for their useful suggestions and comments that greatly improved the manuscript. The authors thank Lorenzo Rook from the University of Florence for his constant support during the making of this work.

Conflicts of Interest: The authors declare no conflict of interest.

References

1. Andersson, M. *Sexual Selection*; Princeton University Press: Princeton, FL, USA, 1994.
2. Berger, J.; Cunningham, C. *Bison: Mating and Conservation in Small Populations*; Columbia University Press: New York, NY, USA, 1994.
3. Janis, C. Evolution of horns in ungulates: Ecology and paleoecology. *Biol. Rev.* **1982**, *57*, 261–318. [CrossRef]
4. Jarman, P. Mating system and sexual dimorphism in large, terrestrial, mammalian herbivores. *Biol. Rev. Camb. Philos. Soc.* **1983**, *58*, 485–520. [CrossRef]
5. Groves, C. Phylogeny of the living species of rhinoceros. *J. Zool.Syst. Evol.* **1982**, *21*, 293–313. [CrossRef]
6. Guérin, C. *Les Rhinoceros (Mammalia, Perissodactyla) du Miocène Terminal au Pleistocène Supérieur en Europe Occidentale Comparaison avec les Espèces Actuelles*; Département des Sciences de la Terre, Université Claude-Bernard: Lyon, France, 1980; pp. 27–43.
7. Pocock, R.I. A sexual difference in the skulls of Asiatic rhinocheroses. *Proc. Zool. Soc. Lond.* **1946**, *115*, 319–322.
8. Owen-Smith, R.M. *Megaherbivores: The Influence of Very Large Body Size on Ecology*; Cambridge University Press: Oakleigh, Australia, 1988.
9. Rachlow, J.L.; Berger, J. Conservation implications of patterns of horn regeneration in dehorned white rhinos. *Conserv. Biol.* **1997**, *11*, 84–91. [CrossRef]
10. Deng, T. Cranial ontogenesis of *Chilotherium* (Perissodactyla, Rhinocerotidae). In *Proceedings of the Eighth Annual Meeting of the Chinese Society of Vertebrate Paleontology*; China Ocean Press: Beijing, China, 1 October 2001; Volume 8, pp. 101–112.
11. Deng, T. New discovery of *Iranotherium morgani* (Perissodactyla, Rhinocerotidae) from the late Miocene of the Linxia Basin in Gansu, China, and its sexual dimorphism. *J. Vertebr. Paleontol.* **2005**, *25*, 442–450. [CrossRef]
12. Lambert, W.D. The Fauna and Paleoecology of the Late Miocene Moss Acres Racetrack Site, Marion County, Florida. Ph.D. Thesis, University of Florida, Gainesville, FL, USA, 1994; 365p.
13. Lu, X.; Deng, T.; Zeng, X.; Li, F. Sexual Dimorphism and Body Reconstruction of a Hornless Rhinocerotid, *Plesiaceratherium gracile*, From the Early Miocene of the Shanwang Basin, Shandong, China. *Front. Ecol. Evol.* **2000**, *8*, 13. [CrossRef]
14. Matthew, W.D. A review of the rhinoceroses with a description of *Aphelops* material from the Pliocene of Texas. *Bull. Univ. Calif. Dep. Geol. Sci.* **1932**, *20*, 411–480.
15. Mead, A.J. Sexual dimorphism and paleoecology in *Teleoceras*, a North American rhinoceros. *Paleobiology* **2000**, *26*, 689–706. [CrossRef]

16. Mihlbachler, M.C. Linking sexual dimorphism and sociality in rhinoceroses: Inisghts frp, *Teleoceras proterum* and *Aphelops malacorhinus* from the Late Miocene of Florida. *Bull. Fla. Mus. Nat. Hist.* **2005**, *45*, 495–520.
17. Mihlbachler, M.C. Sexual Dimorphism and Mortality Bias in a Small Miocene North American Rhino, *Menoceras arikarense*: Insights into the Coevolution of Sexual Dimorphism and Sociality in Rhinos. *J. Mammal. Evol.* **2007**, *14*, 217–238. [CrossRef]
18. Osborn, H.F. A complete skeleton of *Teleoceras fossiger*: Notes upon the growth and sexual characteristics. *Bull. Am. Mus. Nat. Hist.* **1898**, *10*, 51–59.
19. Peterson, O.A. The American diceratheres. *Mem. Carnegie Mus.* **1920**, *7*, 399–477. [CrossRef]
20. Cerdeño, E.; Sánchez, B. Intraspecific variation and evolutionary trends of *Alicornops simorrense* (Rhinocerotidae) in Spain. *Zool. Scr.* **2000**, *29*, 275–305. [CrossRef]
21. Chen, S.; Deng, T.; Hou, S.; Shi, Q.; Pang, L. Sexual dimorphism in perissodactyl rhinocerotid *Chilotherium wimani* from the late Miocene of the Linxia Basin (Gansu, China). *Acta Palaeontol. Pol.* **2010**, *55*, 587–597. [CrossRef]
22. Borsuk-Bialynicka, M. Studies on the Pleistocene rhinoceros *Coelodonta antiquitatis* (Blomenbach). *Palaeontol. Pol.* **1973**, *29*, 5–95.
23. Mihlbachler, M.C. Demography of late Miocene rhinoceroses (*Teleoceras proterum* and *Aphelops malacorhinus*) from Florida: Linking mortality and sociality in fossil assemblages. *Paleobiology* **2003**, *29*, 412–428. [CrossRef]
24. Loose, H. Pleistocene Rhinocerotidae of W. Europe with reference to the recent two-horned species of Africa and S.E. *Scr. Geol.* **1975**, *33*, 1–60.
25. Mazza, P.; Sala, B.; Fortelius, M. A small latest Villafranchian (late Early Pleistocene) rhinoceros from Pietrafitta (Perugia, Umbria, Central Italy), with notes on the Pirro and Westerhoven rhinoceroses. *Palaeontogr. Ltalica* **1993**, *80*, 25–50.
26. Pandolfi, L.; Bartolini-Lucenti, S.; Cirilli, O.; Bukhsianidze, M.; Lordkipanidze, D.; Rook, L. Paleoecology, biochronology, and paleobiogeography of Eurasian Rhinocerotidae during the Early Pleistocene: The contribution of the fossil material from Dmanisi (Georgia, Southern Caucasus). *J. Hum. Evol.* **2021**, *156*, 1–13. [CrossRef]
27. Mihlbachler, M.; Lucas, S.; Emry, R. The holotype specimen of *Menodus giganteus* and the "insoluble" problem of Chadronian brontothere taxonomy: New Mexico. *Mus. Nat. Hist. Sci. Bull.* **2004**, *26*, 129–135.
28. Sall, J.; Lehman, A. *JMP Start Statistics: A Guide to Statistics and Data Analysis Using JMP and JMP IN Software*; Duxbury: New York, NY, USA, 1996.
29. Bryant, D. Age-frequency profiles of micromammals and population density dynamics of *Proheteromys floridanus* (Rodentia) from the early Miocene Thomas Farm site, Florida (U.S.A.). *Palaegeogr. Palaeoclimatol. Palaeoecol.* **1991**, *85*, 1–14. [CrossRef]
30. SAS Institute Inc. *User Guide: Statistics*; SAS Institute Inc.: Cary, NC, USA, 1985.
31. R Foundation. *R: A Language and Environment for Statistical Computing*; R Foundation for Statistical Computing: Vienna, Austria, 2020. Available online: https://www.R-project.org/ (accessed on 5 April 2022).
32. Kieslich, P.; Henninger, F.; Wulff, D.; Haslebeck, J.; Schulte-Mecklenbeck, M. Mouse-tracking: A practical guide to implementation and analysis. In *A Handbook of Process Tracing Methods*; Schulte-Mecklenbeck, M., Kühberger, A., Johnson, J., Eds.; Routledge: New York, NY, USA, 2019; pp. 111–130.
33. Wickham, H. *ggplot2: Elegant Graphics for Data Analysis*; Springer: New York, NY, USA, 2016.
34. Thenius, E. Die verknöcherte Nasenscheidewand bei Rhinocerotiden und ihr systematischer Wert. Zum Geschlechtsdimorphismus fossiler Rhinocerotiden. *Schweiz. Palaeontol. Abh.* **1955**, *71*, 1–17.
35. Azzaroli, A. Rinoceronti pliocenici del Valdarno Inferiore. *Palaeontogr. Ital.* **1962**, *57*, 11–20.
36. Pandolfi, L.; Cerdeño, E.; Codrea, V.; Kotsakis, T. Biogeography and chronology of the Eurasian extinct rhinoceros *Stephanorhinus etruscus* (Mammalia, Rhinocerontidae). *C. R. Palavol.* **2017**, *16*, 762–773. [CrossRef]
37. Dinerstein, E. *The Return of the Unicorns: The Natural History and Conservation of the Greater One-Horned Rhinoceros*; Columbia University Press: New York, NY, USA, 2003.
38. Dinerstein, E.; Price, L. Demography and Habitat Use by Greater One-Horned Rhinoceros in Nepal. *J. Wildl. Manag.* **1991**, *55*, 401–411. [CrossRef]
39. van Strien, N.J. *The Sumatran Rhinoceros in the Gunung Leuser National Park, Sumatra, Indonesia; Its Distribution, Ecology and Conservation*; Privately Published: Doorn, The Netherlands, 1985.
40. Guérin, C.; Heintz, E. *Dicerorhinus etruscus* (Falconer, 1859), Rhinocerotidae, Mammalia, du Villafranchien de La Puebla de Valverde (Ternel, Espagne). *Bull. Du Mus. D'histoire Nat. Paris* **1971**, *18*, 13–22.
41. Lacombat, F. Les Rhinocéros fossiles des sites préhistoriques de l'Europe méditerranéenne et du Massif central, paléontologie et implications biochronologiques. *Brit. Archeol. Rep.* **2005**, *1419*, 1–175.
42. Fortelius, M.M. *Stephanorhinus* (Mammalia:Rhinocerotidae) of the Western European Pleistocene, with a revision of *S. etruscus* (Falconer, 1868). *Palaeontogr. Ital.* **1993**, *80*, 63–155.
43. Guérin, C. Les rhinocéros (Mammalia, Perissodactyla) du gisement villafranchien moyen de Saint-Vallier (Drôme). *Geobios* **2004**, *37*, 259–278. [CrossRef]
44. Ruiz-Bustos, A. Estudio de unos restos de *Dicerorhinus etruscus*, Falconer, encontrados en Granada. *Cuadernos Cienc. Biol.* **1973**, *2*, 2–89.
45. Santafe-Llopis, J.V.; Casanovas-Cladellas, M.L. *Dicerorhinus etruscus brachycephalus* (Mammalia, Perissodactyla) de los yacimientos pleistocénicos de la cuenca Guadix-Baza (Venta Micena y Huéscar) (Granada, España). *Paleont. Evol. Mem. Esp.* **1987**, *1*, 237–254.
46. Cerdeño, E. Revisión de la Sistemática de los Rinocerontes del Neógeno de España. Ph.D. Thesis, Universidad Complutense de Madrid, Madrid, Spain, 1984; 429p.